Chapter 3

Fabrication

3.1 Photolithography

In IC industry, pattern transfer from photomasks onto thin films is achieved exclusively via photolithography. Accurate registration and exposure of a series of successive patterns lead to complex multilayered structures. Photolithography matured rapidly and has become better and better to resolve smaller and smaller features. Research in high aspect ratio photoresist to satisfy the needs of microfabrication also enhance the capacity of photolithography to cover wide ranges of topography.

Photolithography is used to transfer specific patterns from photomask onto a resist-coated wafer. The patterns are defined on a mask and are optically transferred to a photoresist-coated wafer by an exposure system. The dimension of the patterns on the photoresist can be reduced by a factor that depends on the exposure system (contact or project aligner.). After the exposed photoresist was developed, the patterns in the photoresist can be further transferred to the substrate by an etching process. Fig. 3-1 shows a detailed fabrication process of microlenses by photolithography. The process includes cleaning, PR coating, UV exposure with contact aligner, develop, fixing, reflow, and RIE etching.

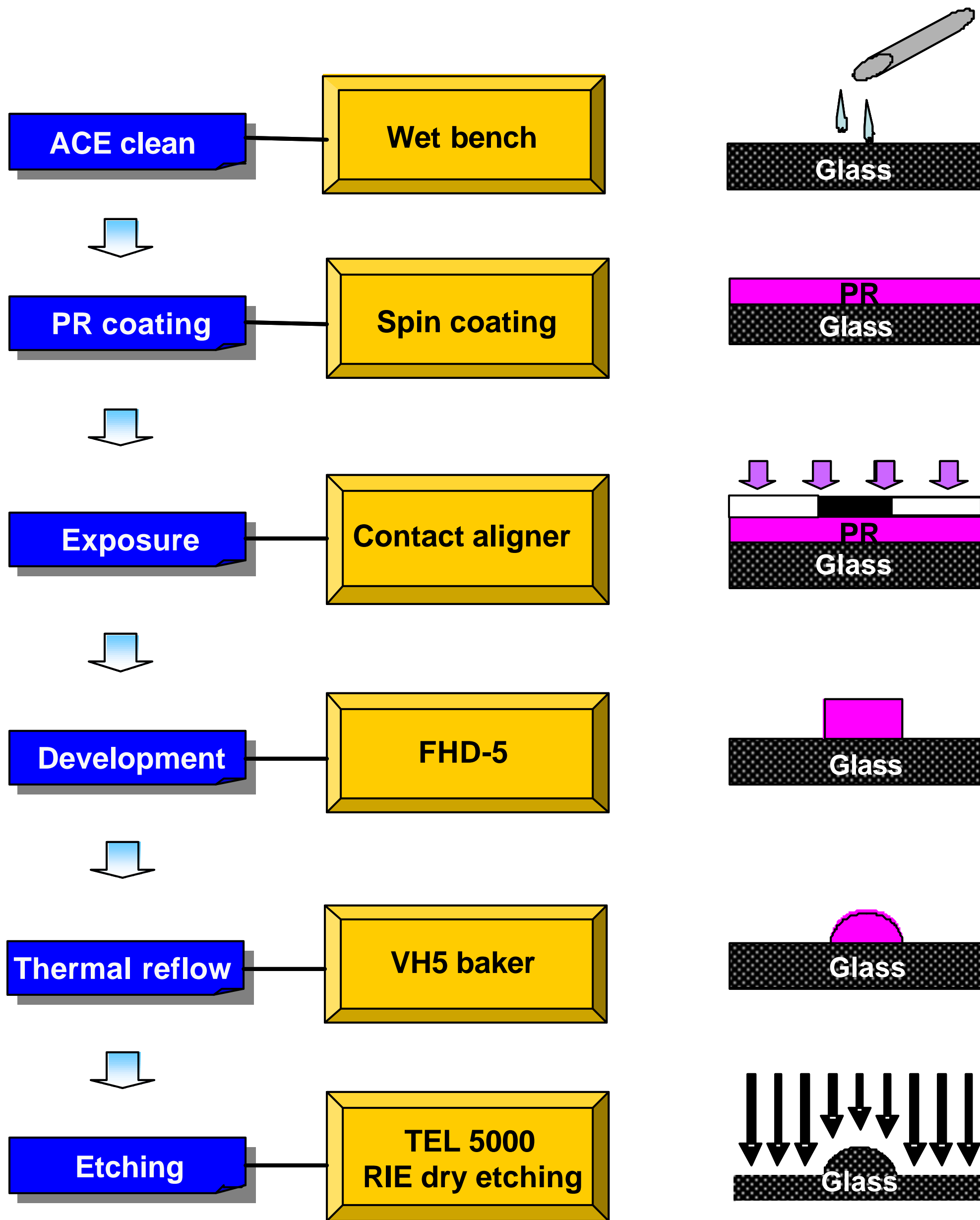

Fig. 3-1 Detail process of photolithography to fabricate the microlens

3.2 Fabrication of 45° mirror

3.2.1 Fabrication process

The fabrication process of such a (110)-groove and 45° mirror is illustrated in Fig. 3-2. First, a 1.2 μm SiO_2 protective layer is thermally grown upon the silicon substrate. It is used as the etching mask because of its extreme low etching rate in the KOH/IPA solution. Then a rectangular PR pattern is opened at 45 °with respect to the primary <110> wafer flat. The pattern is transferred to the SiO_2 mask by dipping in B.O.E for 12 minutes at an etching rate of 0.1 μm per minute. The sample is then immersed in acetone to remove the photoresist. Then the sample is etched in KOH/IPA solution to form the desired mirror and groove. Finally, 300 nm thick Al film is coated to increase the reflectivity of 45 °mirror. The coated Al film consists of 99% aluminum and 1% chromium to prevent oxidation. The etching stop mechanism is time stop method. The desired etching depth should be decided first (125 μm for our design), and the needed etching time can be obtained from the measured etching rate in the KOH/IPA solution.

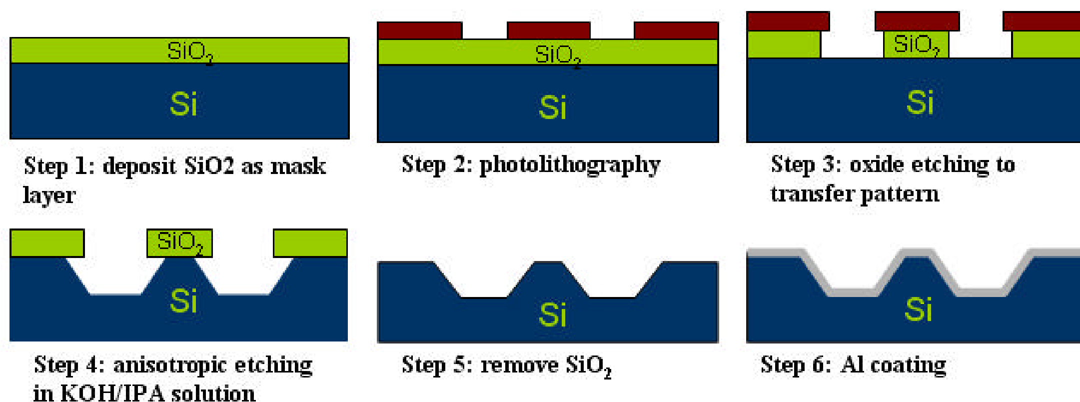

Fig. 3-2 Fabrication process of the V-groove chip

3.2.2 Mask design

The single mode fiber used in the pickup is 125 μm in diameter. To prevent the fiber from rolling on the bottom when it is placed in the groove, the bottom has to be 51.78 μm in width, as illustrated in Fig. 3-3.

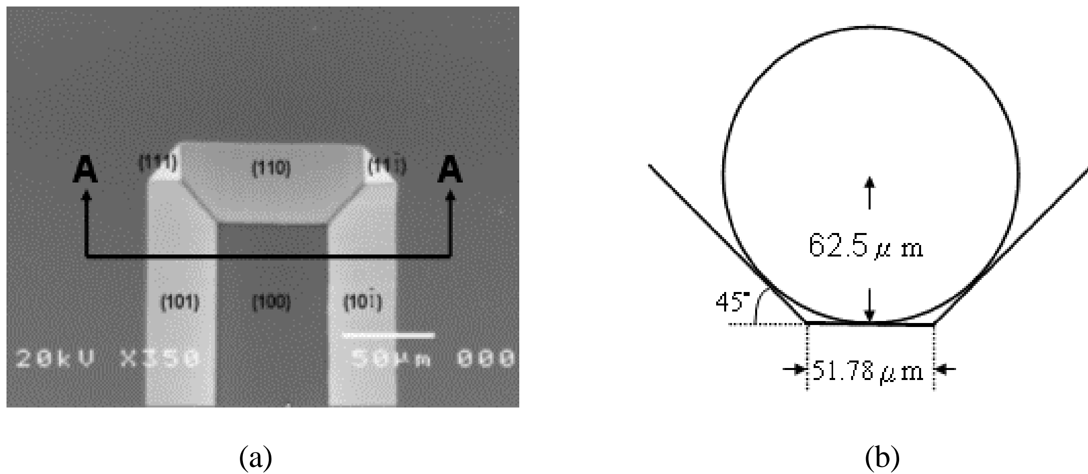

(a) (b)

Fig. 3-3 (a) top view and (b) A-A cross section of V-groove

To achieve a groove of 51.78 μm wide in bottom and 125 μm deep as shown in Fig. 3-4, the width of the etching mask pattern is determined by the selectivity of (110)/(100) planes and the bottom width. In our design, the etching rate of the (100) planes at 41 wt% and 65°C is 23 μm/hr while that of the (110) planes is 4.5 μm/hr. The selectivity is about 1/5.

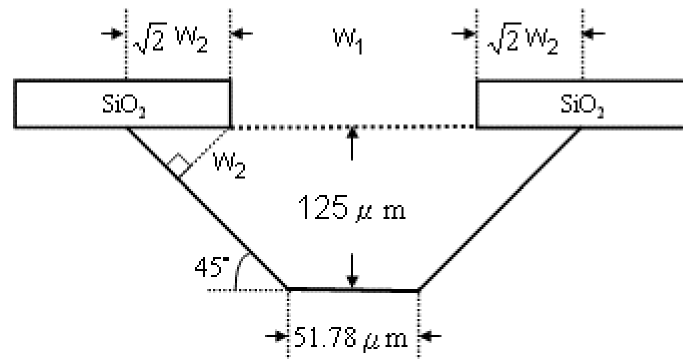

Fig. 3-4 Schematic of the V-groove and etching mask

Since the desired depth is 125 μm and the selectivity is 1/5, $w_2 = 125 \div 5 = 25$ μm. The width of etching mask $w_1 = (51.78 + 125 \times 2) - 2(\sqrt{2} \times w_2) = 231$ μm. Therefore, the mask opening pattern is 231 μm wide and aligned at 45 °to the (110) flat, as shown in Fig. 3-5. Then the sample was put into 41 wt% of KOH/IPA aqueous solution and etched at 65°C for 125μm ÷23μm = 5.43 hours. A fiber groove with proper dimension and extreme smooth 45 °mirror was realized.

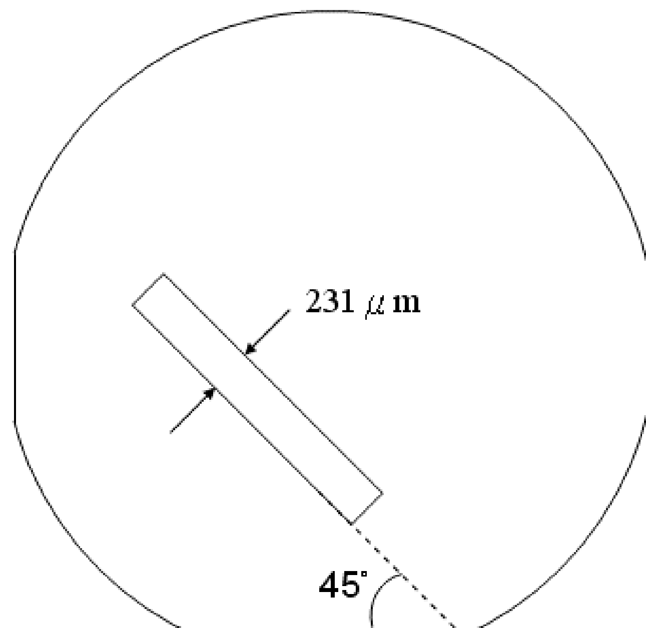

Fig. 3-5 Orientation and width of the pattern opened on (100)-wafer

3.2.3 Etching mask material

To fabricate microstructures on the silicon substrate, the pattern has to be defined on the etching mask. The material of the etching mask should possess the following properties:

1. Chemical stability in the etchant and enough thickness to prevent the attacking from etchant during etching process.
2. Good adhesion with silicon substrate.
3. No pinholes and scratches to prevent the etchant from making incursions into the substrate.

Common etching mask materials for silicon micromaching are:

1. Silicide : SiO_2, Si_3N_4, SiC, etc.
2. Metal : Au, Cr, Ta, W, Al, Pt, Ag, Cu, etc.
3. Organic chemical compound : photoresist.

The etching rate of LPCVD Si_3N_4 in KOH/IPA solution is almost zero, and the adhesion with Si is very excellent. However, Si_3N_4 films have high density of pinholes or scratches. Since the process of metal or SiC is not universal and the photoresist would be lifted-off or decomposed in the anisotropic etchants, such etching masks are not popular in wet anisotropic etching. Due to the dense structure and the extreme low etching rate of SiO_2 in KOH/IPA aqueous solution ($R_{SiO_2} : R_{100} \sim 1 : 200$), a thermally grown 1.2μm thick SiO_2 in steam at 1000℃ in chosen as the protective etching mask layer.

3.3 Measurement system

A scanning electron microscope (SEM) and an atomic force microscope (AFM) were used to inspect the fabricated micro-optical components.

3.3.1 Scanning Electron Microscope (SEM)

Scanning electron microscope (SEM) is an essential instrument to measure the accuracy and fidelity of the fabricated micro-optical structure. The diameter of the electron beam can be focused to a dimension of 10^{-3} μm with an electromagnetic lens. Secondary electrons generated from the area bombarded by the focused electrons are detected as the signal. Simultaneously, the focusing electron beam scans the surface of sample with the aid of scanning coil to map the feature of the measured area, as shown in Fig.3-6.

In our work, a HITACHI S-5700 SEM was used to measure the fabricated structure. The line width, etching depth, and surface uniformity can be accurately measured. SEM was also used to obtain images of the structure.

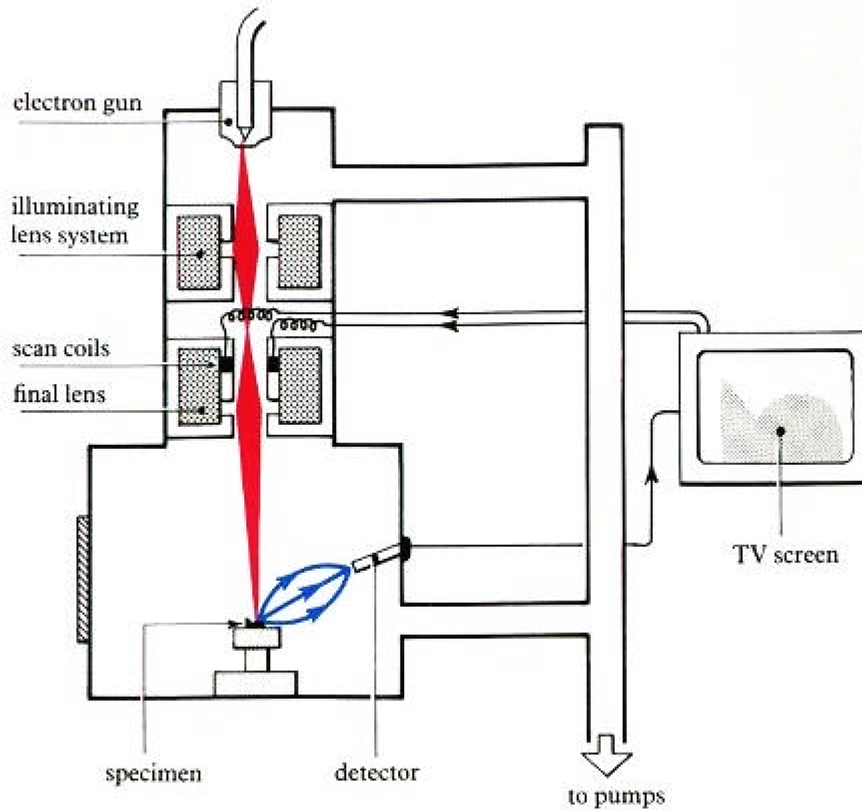

Fig. 3-6 Schematic diagram of scanning electron microscope

3.3.2 Atomic Force Microscope (AFM)

An atomic force microscope consists of a sharp scanning tip at the end of a flexible cantilever. The tip scans across a sample surface while maintaining a small, constant force. The tips typically have an end radius of 2nm to 20nm, depending on tip type. The scanning is actuated by a piezoelectric tube scanner which scans the tip in a raster pattern with respect to the sample (or scans to the sample with respect to the tip). The tip-sample interaction is monitored by reflecting a laser off the back of the cantilever into a split photodetector. By detecting the difference in the photo detector output current, changes in the cantilever deflection or oscillation amplitude are determined. A schematic diagram of this mechanism is shown in Fig. 3-7.

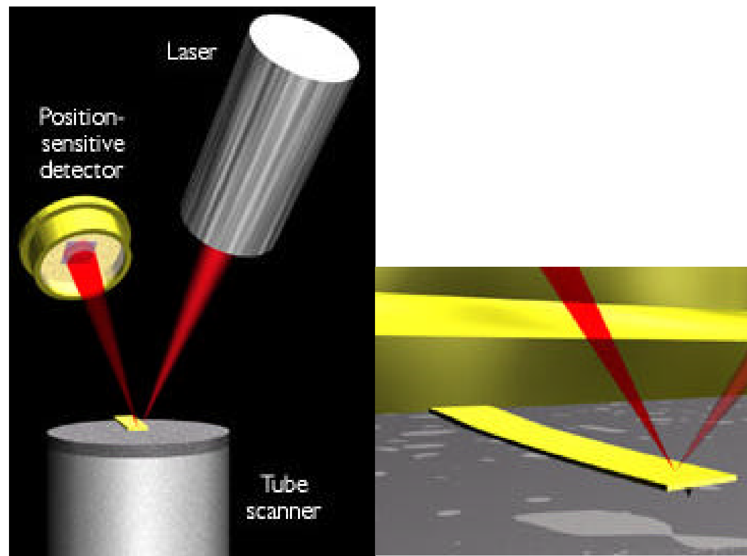

(a) (b)

Fig. 3-7 Concept of AFM and the optical lever: (a) the optical lever; (b) a cantilever touching a sample

Two most commonly used modes in AFM operation are contact mode and tapping mode. Contact mode AFM consists of scanning the probe across a sample surface while monitoring the change in cantilever deflection with the split photodiode detector. A feedback loop maintains a constant cantilever deflection by vertically moving the scanner to maintain a constant photodetector difference signal. The vertical movement of the scanner at each (x,y) location is stored by the computer to form the topographic image of the sample surface. This feedback loop maintains a constant force during imaging, which typically ranges between 0.1 to 100nN.

Tapping mode AFM consists of oscillating the cantilever at its resonance frequency (typically ~300kHz) and lightly "tapping" on the surface during scanning. The laser deflection method is used to detect the root-mean-square (RMS) amplitude of cantilever oscillation. A feedback loop maintains a constant oscillation amplitude

by moving the scanner vertically at every (x,y) location. Recording this vertical movement forms the topographical image. The advantage of tapping mode over contact mode is that it eliminates the lateral shear forces present in contact mode. This enables the tapping mode to image soft, fragile, and adhesive surfaces without damaging them.

3.4 45° mirror

A typical KOH/IPA anisotropic etching result with the mask aligned at 45 ° from the (110) flat is shown in Fig. 3-8. The {110} planes are etched relatively slow in KOH/IPA solution, so they appear as V-grooves very much like the {111} grooves. The difference between the {110} grooves and the {111} grooves is that the {110} planes are etched with a small but finite etch rate while the {111} planes act as etching stop planes. The sidewalls and the ends of the grooves have an angle of 45 °to the surface. The sidewalls act as aligning planes for the fiber and the ends of the groove act as mirrors. Because of the etching of the {110} planes, {111} planes appear in the ends of the grooves between the mirror and the sidewalls, as shown in Fig. 3-8. This results in a decreasing width of the mirror during etching. After a long period of etching time, the (110) mirror would move backward and become narrower and narrower. Finally, the mirror will vanish and the {111} planes will be completely revealed.

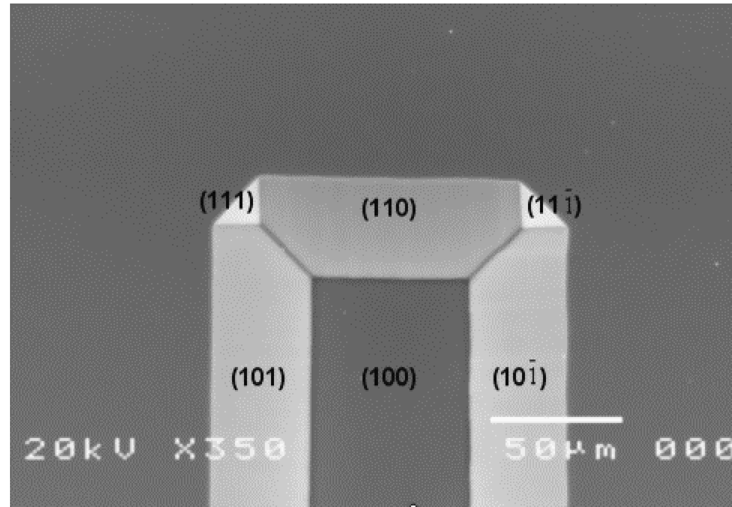

Fig. 3-8 SEM photograph of the end of a {110} groove on (100) silicon with appearing {111} planes

The most important property of the 45° mirror is the surface roughness. It is strongly dependent on KOH concentration, etching temperature, etching depth, etching time and even stirring. The surface roughness was observed and analyzed by an atomic force microscope (AFM) described above. Without stirring, the reaction is limited by diffusion. The reaction products will be accumulated on the surface and lead to a provisional micromask if the diffusion rate is smaller than the reaction rate. It will cause non-uniform etching rate and lead to a rough surface. To improve the smoothness of the etched surface, a magnetic stirrer was put into the aqueous solution to maintain a stable etching. The measured surface roughness with and without stirring is shown in Table. 3-1.

Table. 3-1 Comparison of the surface roughness in 31wt% KOH at 75°C for 120 mins

Etching condition	75°C without stirring	75°C with stirring
R_{rms} (nm)	35.37	25.69
R_{avg} (nm)	26.14	19.76
R_{peak} (nm)	223.57	150.83

The definitions of the three roughnesses measurement are as follows:

$$R_{avg} = \frac{1}{n}\sum_{i=1}^{n} | Z_i - Z_{avg} | \quad (3\text{-}1)$$

$$R_{rms} = \sqrt{\frac{1}{n}\sum_{i=1}^{n} (Z_i - Z_{avg})^2} \quad (3\text{-}2)$$

$$R_{peak} = Z_{max} - Z_{min} \quad (3\text{-}3)$$

R_{avg} is the average roughness, which is equal to the average value of the difference between all measured height (Z_i) and the average height (Z_{avg}). A schematic of the measurement is shown in Fig. 3-9.

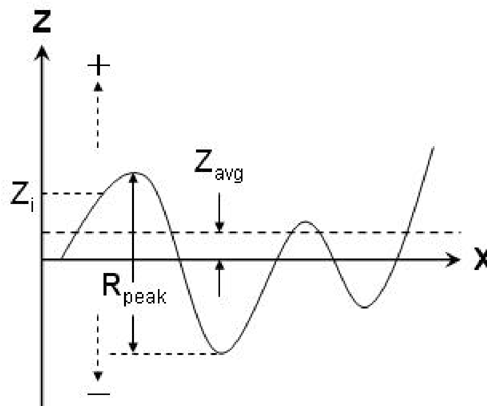

Fig. 3-9 Definition of surface roughness

The smoothness of etched planes can also be improved by using IPA (2-propanol) as an etching additive. The comparison of etching results with and without IPA is shown in Table. 3-2. The other main reason of using IPA as an additive is that (110) planes can be revealed during the etching process. The pure aqueous KOH solution has an etching rate (R_{ijk}) of $R_{110} > R_{100} > R_{111}$. However, the addition of 2-propanol reduces the etching rate for the <100> direction by about 18%, but by almost 90% for the <110> direction. It means that the etching rate between (100) and (110) is reversed, i.e. $R_{100} > R_{110} > R_{111}$. A typical pure KOH aqueous solution etching result is shown in Fig. 3-10. The {110} planes vanish very quickly, only the {111} planes and the {100} vertical sidewalls remain after etching.

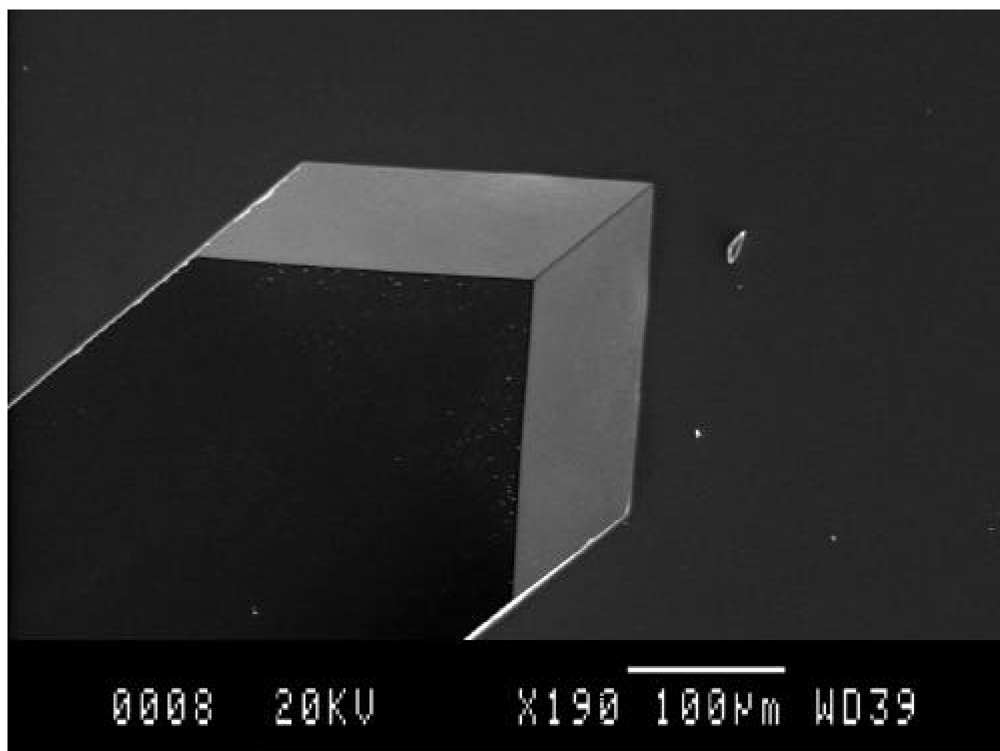

Fig. 3-10 The etching result with no IPA (2-propanol) added

Table. 3-2 Comparison of the surface roughness with and without IPA added in 31 wt% KOH

	75°C	75°C + IPA
R_{rms} (nm)	35.37	28.03
R_{avg} (nm)	26.14	20.41
R_{peak} (nm)	223.57	178.36

The improvement in root mean square, average, and top-to-top roughness was observed with stirring and IPA additive. For microoptical applications, the surface roughness has to be smaller than one-tenth of wavelength of the light source (red light, ? = 632.8nm). For precise optical applications, the value has to be smaller than one-fifteenth of the wavelength (632.8nm ×1/15 = 42.2nm). Therefore, the results in Table. 3-1 need to be improved (R_{peak} = 150.83 ＞ 632.8/10 = 63.28nm). To invest the effect of KOH concentration and etching temperature on the surface roughness, the etching depth was fixed at 100 μm while the KOH concentration was varied from 21% to 51% and the etching temperature was varied from 60°C to 80°C. The volume ratio of IPA and water was 250ml : 1000ml for all experiments, the measured roughness data with an AFM are from more than 150 samples shown in Fig. 3-11.

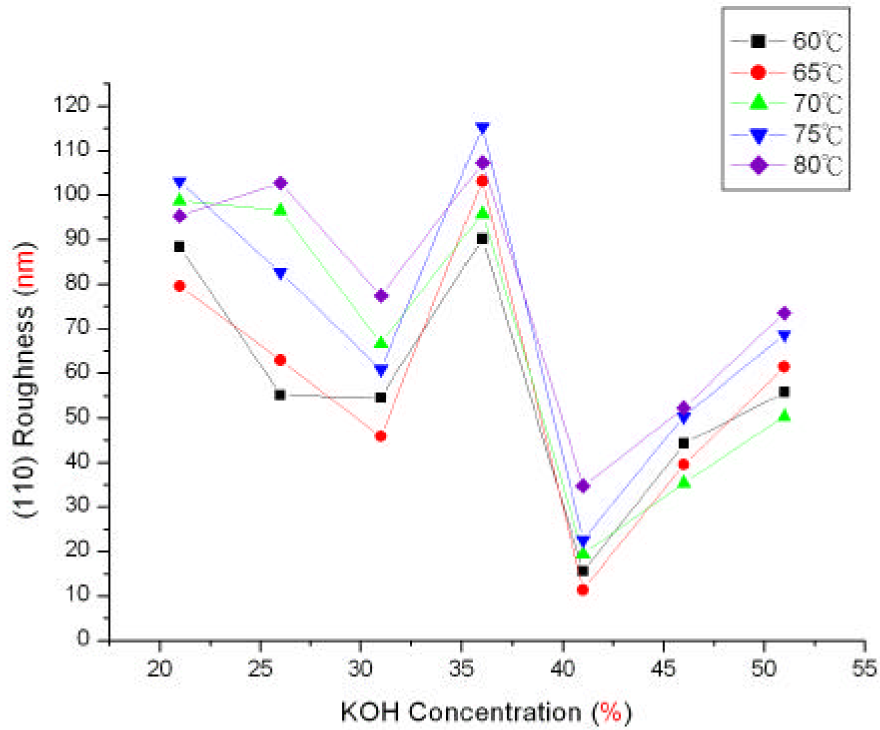

Fig. 3-11 R_{rms} of (110) etched plane (IPA : water = 250ml : 1000ml)

The surface roughness was observed to have a maximum at 36 wt%, 75℃ and a minimum at 41 wt%, 65℃ of the KOH/IPA aqueous solution. Unique surface profiles of etched (110) planes were observed at different KOH concentration. Below 41 wt%, due to the fast etching rate of (110) planes and the more violent attacking action of the KOH/IPA solution, etched planes with wave shape were observed, as shown in Fig. 3-12. Wave shape formed by {111} striation effect side by side is due to that the etching rate of {110} planes is faster than that of {111} at the concentration below 41 wt%. This low concentration (< 41 wt%) will cause ridge structure shown in Fig. 3-13, which will easily deteriorate the flatness of the {110} planes.

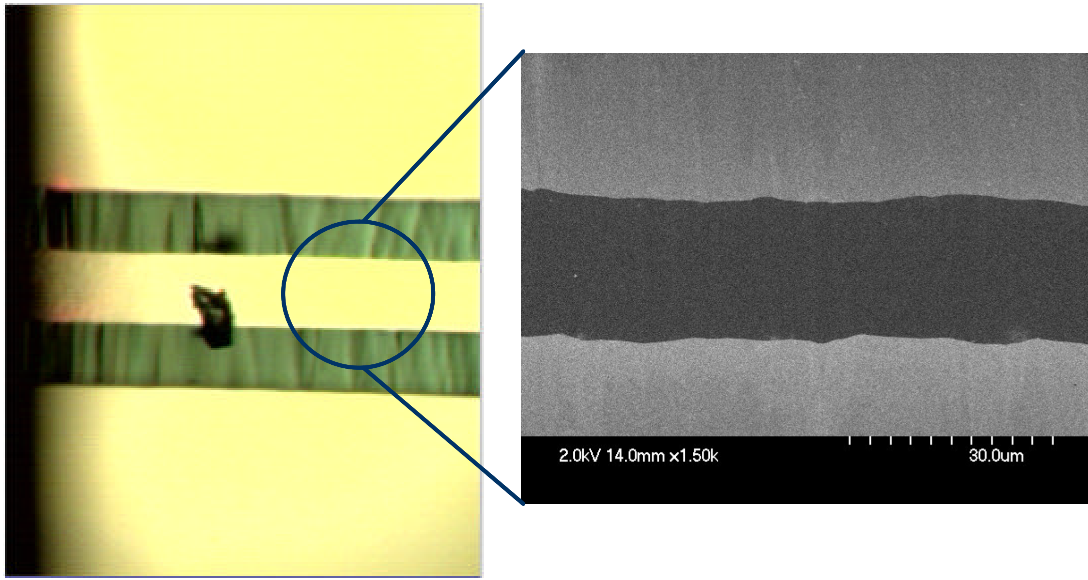

(a) (b)

Fig. 3-12 (a) Optical microscope and (b) SEM photograph of wave shape

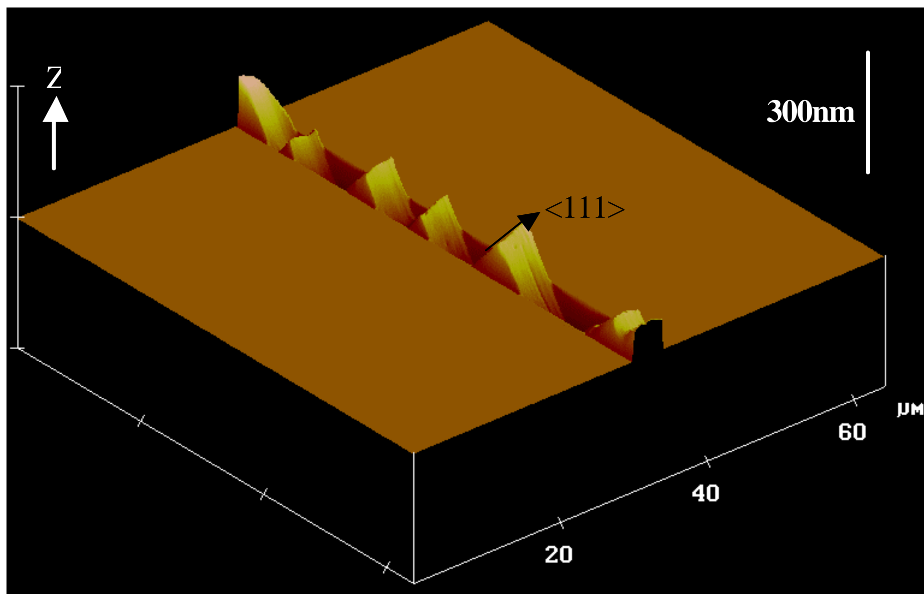

Fig. 3-13 AFM photograph of ridge structure on (110) surface

Above 41 wt%, due to the slower etching rate of (110) planes and weaker attacking action of KOH/IPA solution, hillocks were observed on the (100) etched surface, as shown in Fig. 3-14. The small hillocks are caused by crystal defeats. They can not be removed during weaker reaction. Such small spots would lead to a rough etched surface. The AFM scanning result is shown in Fig. 3-15.

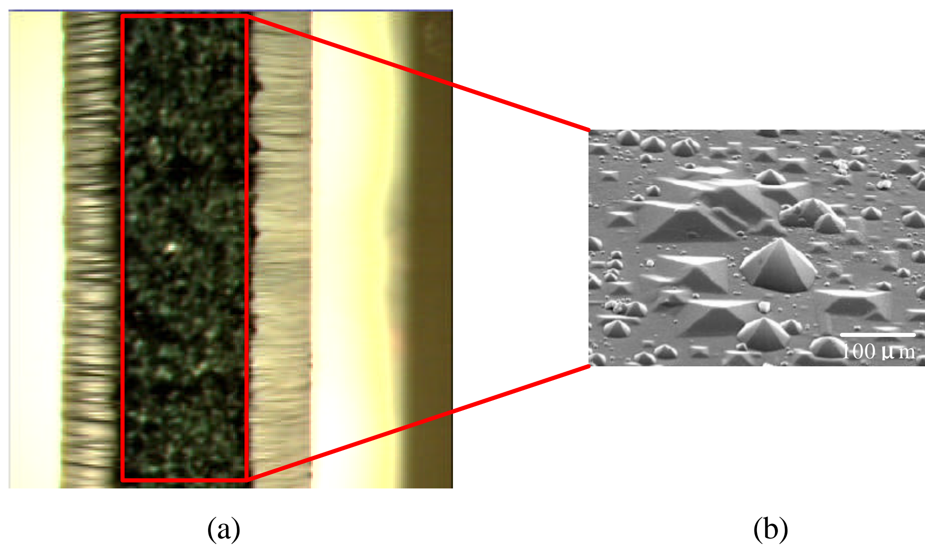

(a) (b)

Fig. 3-14 (a) Optical microscope and (b) SEM photograph of hillocks

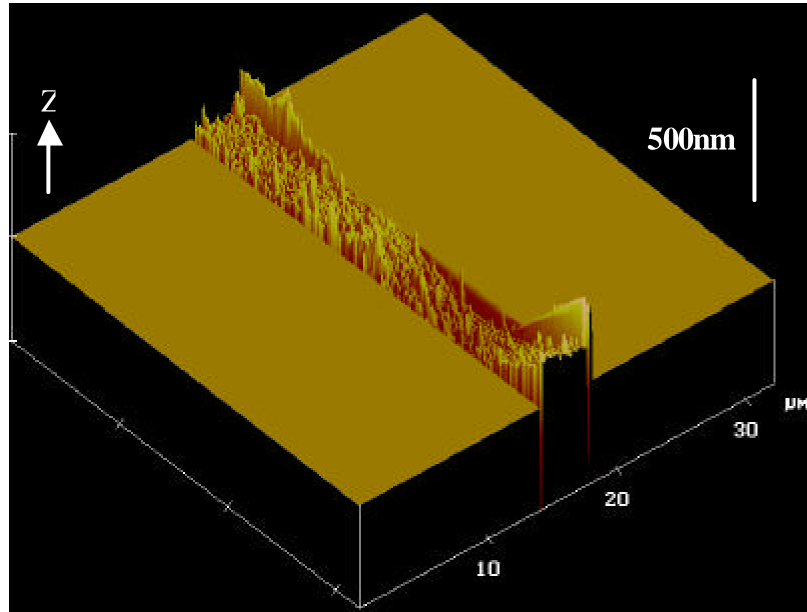

Fig. 3-15 AFM photograph of hillocks on (110) surface

To balance the wave shape and hillock effect, 41 wt% KOH aqueous solutions at 65°C had been chosen for the anisotropic etching. Minimum surface roughness occurred at this condition; the result measured by AFM is shown in Fig. 3-16. The feasibility of the mirror surface can be proved when the local region with laser illumination is extremely small and can be regarded relatively smooth.

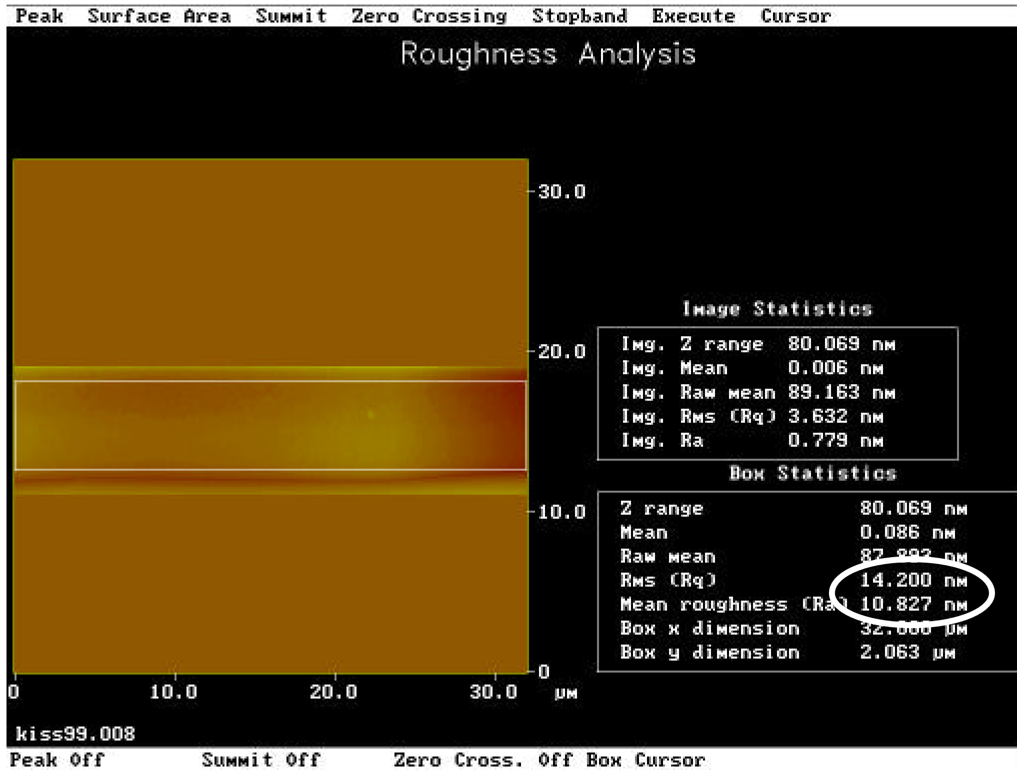

(a)

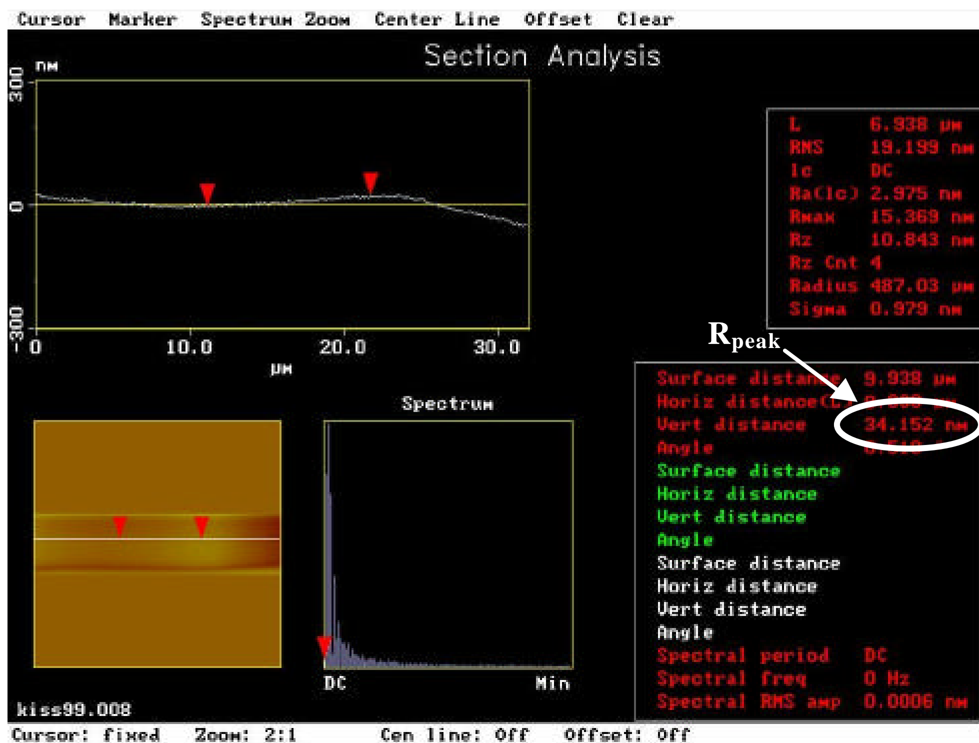

(b)

Fig. 3-16 AFM photograph of (a) (110) surface roughness and (b) top-to-top distance

3.5 Hemispherical-shaped fiberlens

Hemispherical microlenses are fabricated on the SMF (single mode fiber) front end by high-frequency arc discharge method[36]. The fabrication process is schematically illustrated in Fig. 3-17. First, an arc-discharge splicing machine was use to join the SMF and a coreless fiber (silica fiber). Next, the pure silica fiber was cleaved perpendicularly to its axis. The rod length g was controlled with the aid of a microscope eyepiece graticule. When a high-frequency arc discharge is applied, the free end of the silica rod melts and contracts to form a hemisphere due to surface tension (Fig. 3-17 (c)). A side view of the hemispherical lens is shown in Fig. 3-18 (a). The focused spot size of the hemispherical fiberlens, shown in Fig. 3-18 (b), was measured by a CCD. In the case of $\lambda = 0.63$ μm and silica rod distance g ≅ 203 μm, the spot size of full-width at half maximum is 12.5 μm (x-direction) and 13 μm (y-direction)

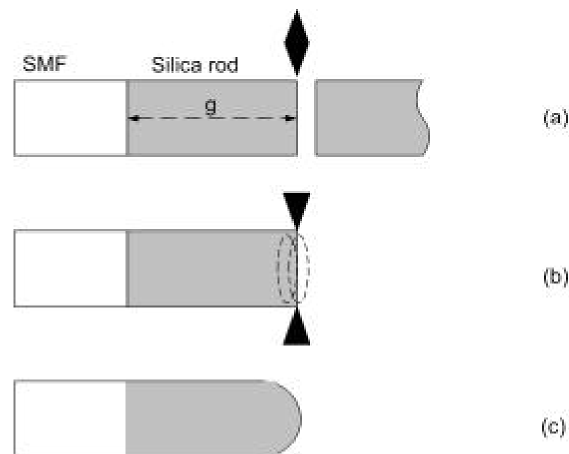

Fig. 3-17 Schematic illustration of the fabrication process for hemispherical-shaped fiberlens.

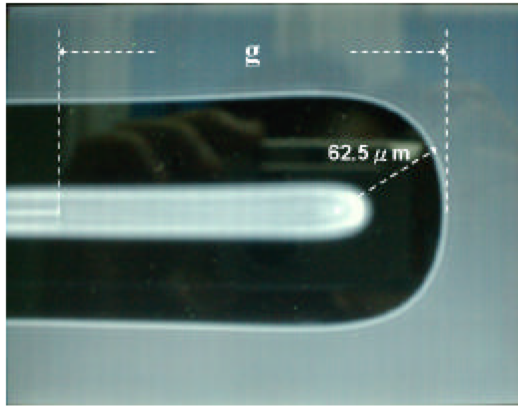

(a)

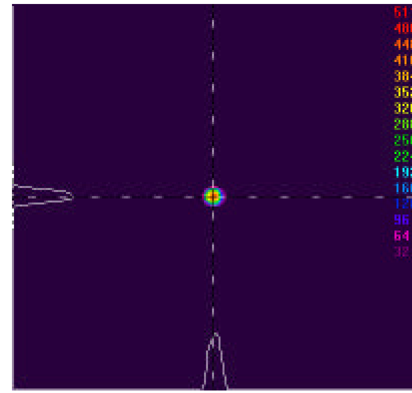

(b)

Fig. 3-18 (a) Side view of the hemispherical lens; (b) measured spot profile (12.5 μm at x-direction, 13 μm at y-direction) for $\lambda = 0.63$ μm and $g \cong 203$ μm

The combination of fiberlens/V-groove is shown in Fig. 3-19. The ends of the groove acts as a 45 ° mirror and changes the light to a right angle when the light is out of the fiber.

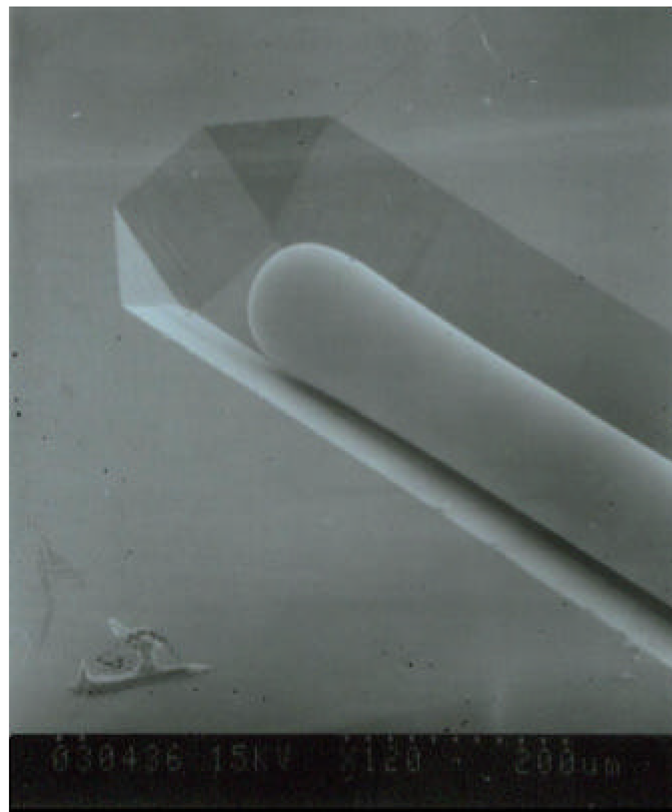

Fig. 3-19 SEM photograph of the combination of fiberlens/V-groove

3.6 Summary

A 45° mirror with extreme smooth plane (R_{rms} = 14.2 nm) has been successfully fabricated and factors that affect the surface roughness has been specified and overcome. A hemispherical-shaped microlens on a single-mode fiber to achieve the focused spot of full-width at half maximum = 12.5 μm (x-direction) and 13 μm (y-direction) using a simple fabrication procedure. This microlens design is easily compatible with the 45° mirror to achieve micro-optical integration. The combination of fiberlens/45° mirror is a potential scheme for volume reduction and readout mechanism for optical data storage applications.